

Single-molecule imaging of individual amyloid protein aggregates in human biofluids

Authors: Mathew H. Horrocks^{1†}, Steven F. Lee^{1†}, Sonia Gandhi², Nadia K. Magdalinou³, Serene W. Chen¹, Michael J. Devine⁴, Laura Tosatto¹, Magnus Kjaergaard^{1,5}, Joseph S. Beckwith¹, Henrik Zetterberg^{2,6}, Marija Iljina¹, Nunilo Cremades¹, Christopher M. Dobson¹, Nicholas W. Wood², David Klenerman¹.

*Affiliations:

¹Department of Chemistry, University of Cambridge, Lensfield Road, Cambridge CB2 1EW, UK.

²Department of Molecular Neuroscience, University College London, Institute of Neurology, Queen Square, London WC1N 3BG, UK.

³Reta Lila Weston Institute of Neurological Studies, University College London, 1 Wakefield Street, London, WC1N 1PJ, UK.

⁴Division of Brain Sciences, Imperial College of London, Hammersmith Hospital, Du Cane Road, London W12 0NN, UK.

⁵Present address: iNANO, Aarhus University, Gustav Wieds Vej 14, DK-8000 Aarhus C, Denmark.

⁶Clinical Neurochemistry Laboratory, Department of Psychiatry and Neurochemistry, Institute of Neuroscience and Physiology, the Sahlgrenska Academy, University of Gothenburg, Mölndal, Sweden.

*Correspondence to: dk10012@cam.ac.uk

†These authors contributed equally to this work.

Supporting Information

Data analysis

For the labeled α S, each data-set consisted of 27 image stacks of 150 frames from both the blue and red channels, measured in different regions of the cover-slide. Data analysis was performed using ImageJ¹; the stacks were first averaged over the 150 frames for each channel and the “Find Maxima” command (based on a plugin contributed by Michael Schmid) was used to detect spots present in the averaged blue channel, and the intensities of the detected spots were then quantified in both the blue and red channels. A standard noise tolerance level was set to differentiate the spots from the background (a change in signal of 1000 fluorescent counts was used as a threshold). For unlabeled samples, stacks only in the blue channel were recorded and analyzed.

In order to distinguish oligomers from fibrils when α S was incubated under aggregating conditions and samples measured, a custom-code in Igor Pro (Wavemetrics) was written. Detected fluorescent spots were fitted to 2D elliptic Gaussians; only those that had fitted widths less than two pixels were classified as oligomers.

The optimum ThT concentration for SAVE imaging

In order to determine the optimum ThT concentration to use for oligomer detection, the enriched oligomers were imaged at a range of ThT concentrations. Figure S1 shows the average number and intensity of the spots detected at different ThT concentrations. As the concentration of ThT increases, the number and intensity of spots detected increases, since more ThT is available to bind to the oligomers. However, at higher concentrations still ($> 5 \mu\text{M}$), the detection efficiency decreases, since the background signal increases more than the signal from single oligomers, leading to a decrease in the signal-to-background ratio. For all experiments, a ThT concentration of $5 \mu\text{M}$ was used.

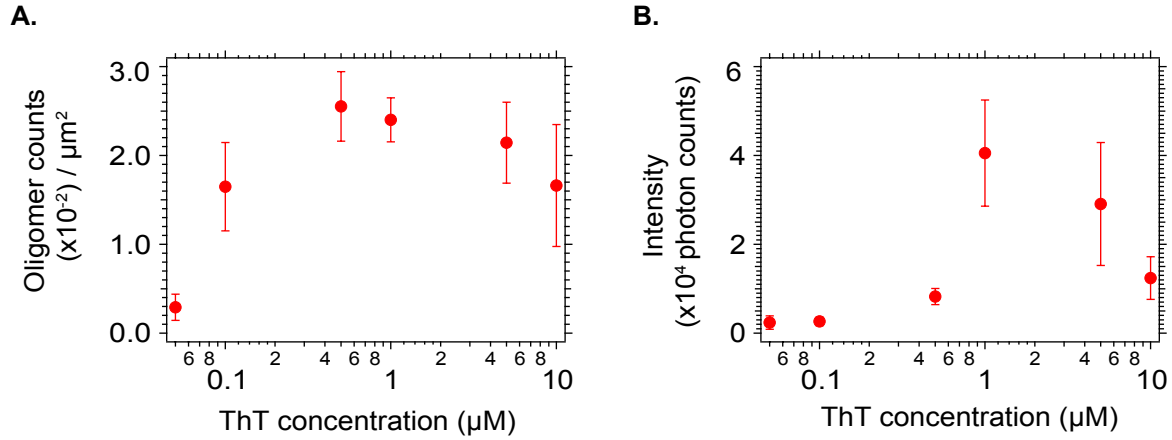


Figure S1. The average number of oligomers detected at varying concentrations of ThT (mean \pm S.D., $n = 9$ images). B. The average intensity of the oligomers detected at each concentration of ThT (mean \pm S.D., $n = 9$ images).

The optimum threshold for spot counting

As mentioned previously, to count the number of species in the resultant images, we used the “Find maxima” command in ImageJ (with a standard noise tolerance level of 1000). This threshold was selected based on its ability to visibly select the majority of puncta in images of the enriched oligomers, without detecting background fluorescence as events. The thresholding was also insensitive to variation in the TIRF illumination across the images. This thresholding was then used for all of the CSF sample images. We attempted using higher thresholds to distinguish between the HCs and PD sample images further; however, with increasing thresholds, the number of events detected decreases exponentially, and the trend then becomes lost in the sampling noise, and so we found that simply using the find maxima command resulted in the least biased method for thresholding.

Patient samples

Table S2. Clinical details of patients with PD, giving the number of aggregates and aggregate brightness (mean from three sets of 3x3 grids \pm S.D.). H-Y - Hoehn & Yahr grade.

Case	Age	Gender	Duration (years)	H-Y Score	Number of aggregates (counts/ μm^2)		Aggregate brightness (photons)	
1	68	Male	20	4	0.0144	\pm 0.0078	3537	\pm 452
2	75	Male	14	4	0.0148	\pm 0.0085	3295	\pm 556
3	58	Male	5.5	2	0.0129	\pm 0.0048	4692	\pm 2086
4	69	Female	11	3	0.0100	\pm 0.0045	3260	\pm 591
5	53	Female	5	1	0.0237	\pm 0.0047	5032	\pm 437
6	60	Male	6	2	0.0148	\pm 0.0061	3552	\pm 355
7	62	Female	15	4	0.0160	\pm 0.0031	5711	\pm 490
8	51	Female	5	1	0.0098	\pm 0.0017	2423	\pm 1274
9	57	Male	1.5	2	0.0112	\pm 0.0026	2980	\pm 337
10	71	Female	15	2	0.0137	\pm 0.0021	3193	\pm 283
11	74	Female	18	3	0.0055	\pm 0.0012	3101	\pm 171
12	65	Male	15	3	0.0177	\pm 0.0069	4165	\pm 1083
13	63	Female	14	3	0.0189	\pm 0.0034	4879	\pm 607
14	63	Male	13	2	0.0088	\pm 0.0012	2644	\pm 358
15	72	Male	17	5	0.0134	\pm 0.0027	3493	\pm 450
16	66	Male	5	2	0.0085	\pm 0.0009	3154	\pm 338
17	68	Male	5	2	0.0027	\pm 0.0009	3802	\pm 215
18	85	Female	14	4	0.0169	\pm 0.0012	3714	\pm 504

Table S3. Clinical details of control subjects, giving the number of aggregates and aggregate brightness (mean from three sets of 3x3 grids \pm S.D.).

Case	Age	Gender	Total aggregates (counts/ μm^2)		Average aggregate brightness (photons)	
19	69	Male	0.0016	\pm 0.0078	2793	\pm 260
20	69	Male	0.0022	\pm 0.008469	3254	\pm 835
21	67	Female	0.0049	\pm 0.0048	5863	\pm 1139
22	64	Female	0.0069	\pm 0.0045	2874	\pm 357
23	64	Male	0.0055	\pm 0.0047	2377	\pm 443
24	63	Male	0.0045	\pm 0.0061	3149	\pm 229
25	61	Female	0.0174	\pm 0.0031	4598	\pm 722
26	76	Male	0.0058	\pm 0.0017	2502	\pm 112
27	62	Male	0.0038	\pm 0.0026	2413	\pm 217
28	71	Male	0.0028	\pm 0.0021	3447	\pm 555
29	71	Male	0.0124	\pm 0.0012	3358	\pm 375
30	64	Female	0.0046	\pm 0.0069	2937	\pm 747
31	46	Female	0.0064	\pm 0.0034	3914	\pm 1234
32	56	Male	0.0044	\pm 0.0012	2867	\pm 335
33	64	Female	0.0072	\pm 0.0027	6470	\pm 150
34	46	Female	0.0026	\pm 0.0009	3484	\pm 76
35	45	Female	0.0026	\pm 0.0009	3376	\pm 625
36	61	Female	0.0043	\pm 0.0012	3406	\pm 134

Supplementary Materials References:

1. Rasband, W.S., ImageJ, U. S. National Institutes of Health, Bethesda, Maryland, USA, <http://imagej.nih.gov/ij/>, 1997-2014.